JOURNAL OF MATERIALS SCIENCE 21 (1986) 3889–3900

Gaseous reduction of Fe_2O_3 compacts at 600 to 1050° C

A. A. EL-GEASSY
Central Metallurgical Research and Development Institute (CMRDI), National Research Centre, Cairo, Egypt

Dense Fe_2O_3 briquettes were isothermally reduced with hydrogen, carbon monoxide and H_2–CO mixtures at 600 to 1050° C. The course of reduction was followed by measuring the oxygen weight loss, as a function of time, using a thermogravimetric technique. Microscopic examination, X-ray and carbon analyses were also used to elucidate the kinetics and mechanisms of reduction of Fe_2O_3 briquettes. In the initial stages of reduction, the highest reduction rate was obtained in hydrogen while the slowest was in carbon monoxide. In CO–H_2 gas mixtures, the rate decreased with increasing amounts of carbon monoxide. In the later stages of reduction, a minimum reduction rate was only observed during the reduction with hydrogen and hydrogen-rich gas mixtures due to the formation of dense γ-iron at 900 to 950° C. This was eliminated in carbon monoxide and carbon-monoxide-rich gas mixtures due to the carbon deposition in the samples and secondary reactions.

1. Introduction

Efforts in the iron and steel industry are now directed towards using reformed natural gas for direct reduction of iron ores. Up to the present time natural gas, which is composed of methane (> 95%), has been the process fuel used in most of the direct reduction plants throughout the world. Natural gas cannot be directly used but must be reformed with either steam or carbon dioxide to produce hydrogen and carbon monoxide [1]. In recent years more detailed studies have been made, both experimentally and theoretically, to gain further understanding of the factors affecting the reduction of iron oxides. Although the gaseous reduction of iron oxides is a complex process, the kinetics and mechanisms of reduction have been reviewed and summarized [2–4]. During reduction of haematite directly to metallic iron, magnetite and wustite are formed, depending on reduction temperature. The presence of these intermediate phases further complicates the reduction mechanism and their structure plays an important role in the whole reduction process. Prosser [5] considers that the structure of oxides, impurities in the solid solution and non-stoichiometry of solids may affect the rate of chemical reactions.

Most investigators have discussed the reduction with either hydrogen [3, 4, 6, 7] or carbon monoxide [7, 8] and relatively little work has been carried out with H_2–CO mixtures which is the main constituent of reformed natural gas. The mechanism by which iron oxides are reduced by carbon monoxide is different from that of hydrogen reduction, although both are temperature dependent [8]. Recently [9–11], the mechanisms and kinetics of reduction of wustite micropellets to iron, which is considered the rate-controlling step in the whole reduction process, with hydrogen, carbon monoxide and H_2–CO mixtures have been studied and discussed. It has been found that a small addition of hydrogen to carbon monoxide greatly increased the rate of reduction, while addition of a small amount of carbon monoxide to hydrogen decreased the rate of reduction due to the poisoning effect of carbon monoxide molecules on the surface of the iron oxide. Some authors observed a reduction-rate minima during the gaseous reduction of iron oxides with hydrogen, carbon monoxide and and H_2–CO mixtures. They attributed it to either physical effects such as sintering and α–γ-iron transformation [6–10] or chemical effects such as formation of fayalite, ferrites and other compounds [12–14].

Opinions differ as to whether the rate-controlling mechanism in the reduction of iron oxides is gaseous diffusion, chemical reaction or a solid-state diffusion process. The reported values of activation energy obtained for gas–solid reactions vary widely from 2 up to 50 kcal mol^{-1} or even higher. The measured values of activation energy may be affected by the influence of temperature on the surface area of solids and on the morphology of product solid. Strongway [15] correlated the values of apparent activation energy obtained in the gaseous reduction of iron oxides with the corresponding rate-controlling mechanism.

The present investigation aims at studying the reduction of Fe_2O_3 briquettes directly to metallic iron with hydrogen, carbon monoxide and their mixtures at a wide range of temperature (600 to 1050° C). In the view of previous work, this will lead to further understanding of the kinetics and mechanism of gaseous reduction of iron oxides.

2. Experimental techniques

2.1. Materials

Reagent-grade Fe_2O_3 powder (< 100 μm). BDH, UK, was used in this investigation. It contains 99.50%

0022–2461/86 $03.00 + .12

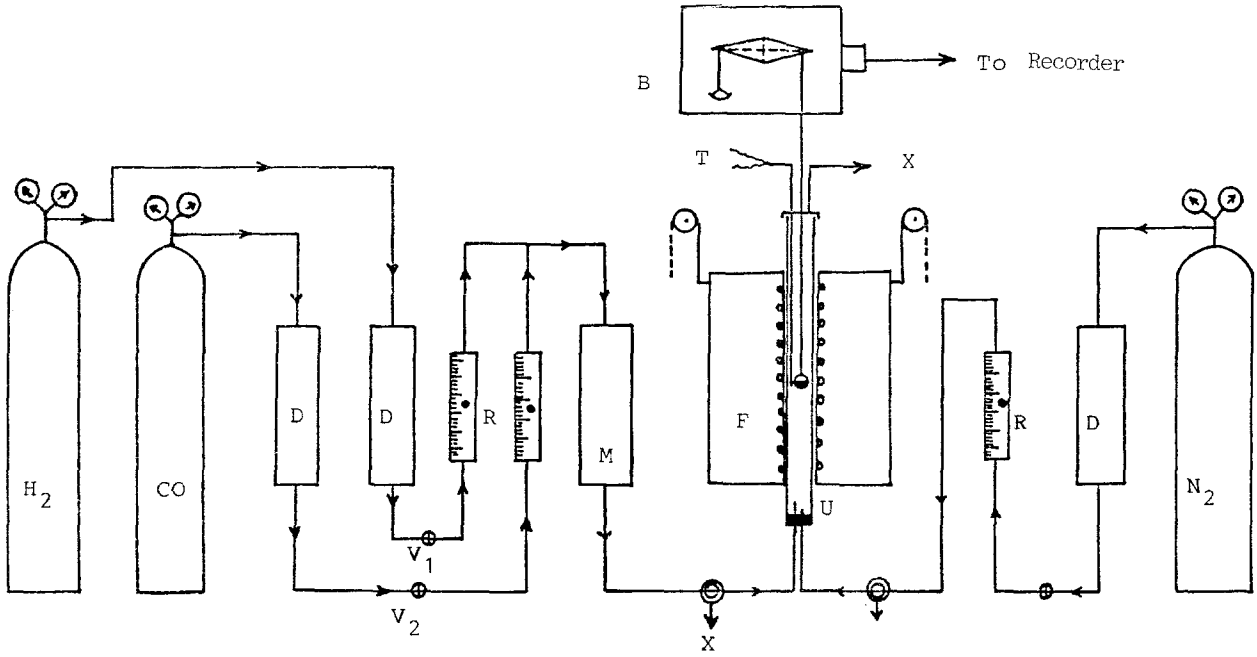

Figure 1 Reduction and gas flow system. B, balance; D, drying towers; F, furnace; M, mixing tower; R, rotameters; T, temperature indicator; U, reaction tube; V, valves; X, to burner.

Fe_2O_3 with the balance being oxides of calcium, magnesium, aluminium and silicon. Briquettes were made by moistening Fe_2O_3 powder with 6% distilled water, then equal weights (4.0 g) were compacted in a cylindrical mould (12.3 mm inner diameter) at 50 kg cm^{-2} using hydraulic press. The height of the produced briquettes was 15.0 mm. These were dried at 110° C, then sintered at 1000° C for 2 h in a muffle furnace. The total porosity of these briquettes was ~ 12%.

The gases used in this study were hydrogen, carbon monoxide, nitrogen, helium and argon. These gases were purified and dried before being introduced to the reduction experiments.

2.2. Reduction tests

A weight loss technique was used for accurate determination of the weight of oxygen loss during reduction experiments. The output of the balance was fed to a strip chart recorder for continuous recording of the weight changes during the reduction as a function of time. The reduction and the gas flow system can be seen in Fig. 1. The Fe_2O_3 briquettes, which hang from the balance in the reaction tube with the aid of Pt/10% Rh basket, were isothermally reduced with hydrogen, carbon monoxide and H_2–CO mixtures. 1000 ml min^{-1} of either hydrogen or carbon monoxide was found to be sufficient to overcome the resistance of the gas-boundary layer around the sample.

Partially or completely reduced samples were examined by scanning electron and light microscopes and an X-ray diffraction technique in order to study the phases formed during reduction. Porosity measurements using an S.K. apparatus [16] were also used. The total amounts of carbon in the reduced samples (iron carbides and graphite) were determined by the aid of a C.S. apparatus (Lybold–Heraus, W. Germany). Graphite was determined by a low-temperature oxidation technique.

3. Results and discussion

The kinetics of reduction of Fe_2O_3 briquettes directly to metallic iron was studied over a wide range of temperature. Reduction was carried out with hydrogen, carbon monoxide and their mixtures. The influence of temperature and reducing gas composition on the reduction rate was investigated. X-ray and carbon analyses together with microscopic examination and porosity measurements were used to elucidate the mechanism of reduction with carbon monoxide and carbon monoxide-containing gas mixtures, it was observed that the recorded oxygen weight loss was less than the calculated value of oxygen in Fe_2O_3 sample. This difference between the calculated and the experimental values of weight loss decreases with rise in temperature. This is due to carbon deposition which resulted from thermal decomposition of carbon monoxide ($2CO \rightleftharpoons C + CO_2$). This carbon increases the weight of the sample leading to false recording of the weight-loss data. This error was correlated by chemical analysis of Fe^{3+}, Fe^{2+}, Fe and C%.

3.1. Influence of temperature

Sintered Fe_2O_3 briquettes (12% total porosity) were isothermally reduced at 600 to 1050° C with pure hydrogen, carbon monoxide and H_2–CO mixtures. The typical reduction curves (% reduction = [weight of O_2 removed at a given time/total calculated weight of O_2 in Fe_2O_3] × 100) with hydrogen, 75% H_2 + 25% CO, 50% H_2 + 50% CO, 25% H_2 + 75% CO and with carbon monoxide are shown in Figs 2 to 6, respectively. It can be seen from these figures that the rate of reduction increased with temperature for a given reducing gas composition at the initial stages of reduction. This is reasonable since the basic principles of chemical thermodynamics and kinetics and the fundamental laws of diffusion would predict that the rate of reduction of iron oxide should

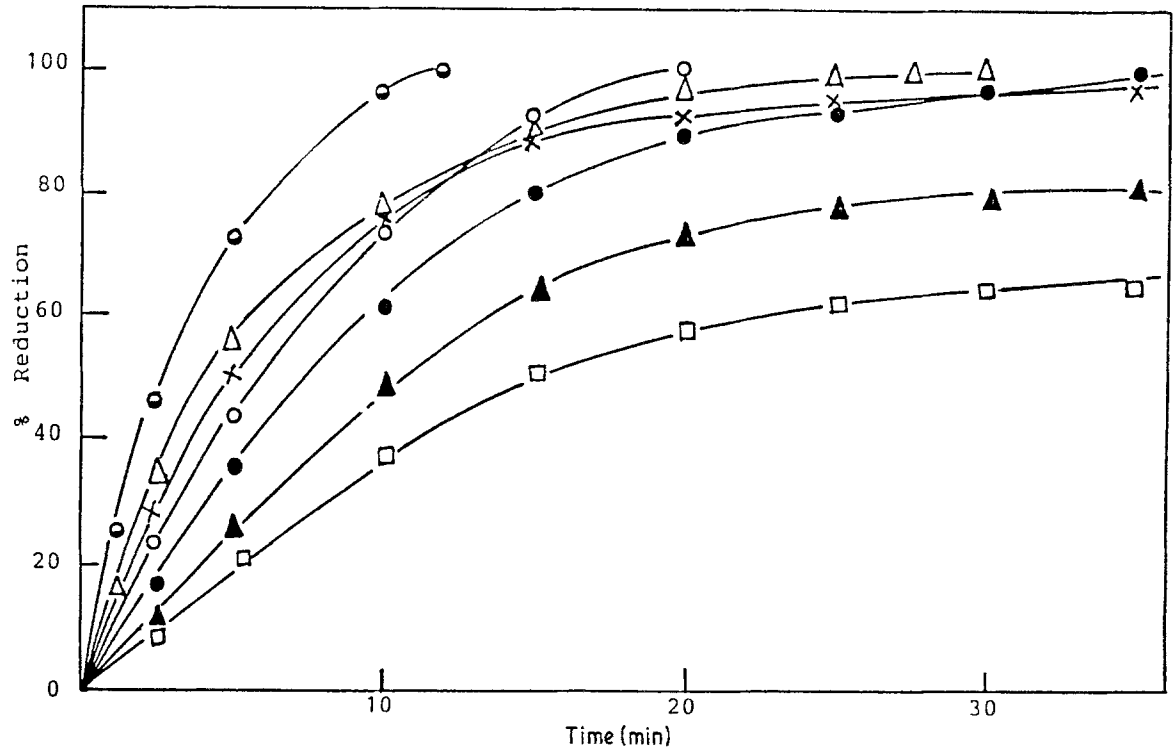

Figure 2 Reduction curves of Fe_2O_3 briquettes with hydrogen. Reduction temperatures (° C): ◒, 1050; △, 1000; x, 950; ○, 900; ●, 800; ▲, 700; □, 600.

increase with temperature. With progress of reduction, after a certain extent, depending on the reducing gas composition, the reduction at 900° C is higher than that at 950 and 1000° C. This slowing down in the rate was only observed in the case of reduction with hydrogen and hydrogen-rich gas mixtures ($> 50\%$ H_2). On the other hand, for the reduction with carbon monoxide and carbon monoxide-rich gas mixtures ($\geqslant 50\%$ CO) no slowing down in the rate was detected over the whole temperature range used. This clearly indicates that the reducing gas composition has a significant effect on the kinetics and the mechanisms of Fe_2O_3 reduction.

3.1.1. Reduction with hydrogen and hydrogen-rich mixture

The reduction of Fe_2O_3 with hydrogen and 75% H_2 + 25% CO gas mixture is shown in Figs 2 and 3,

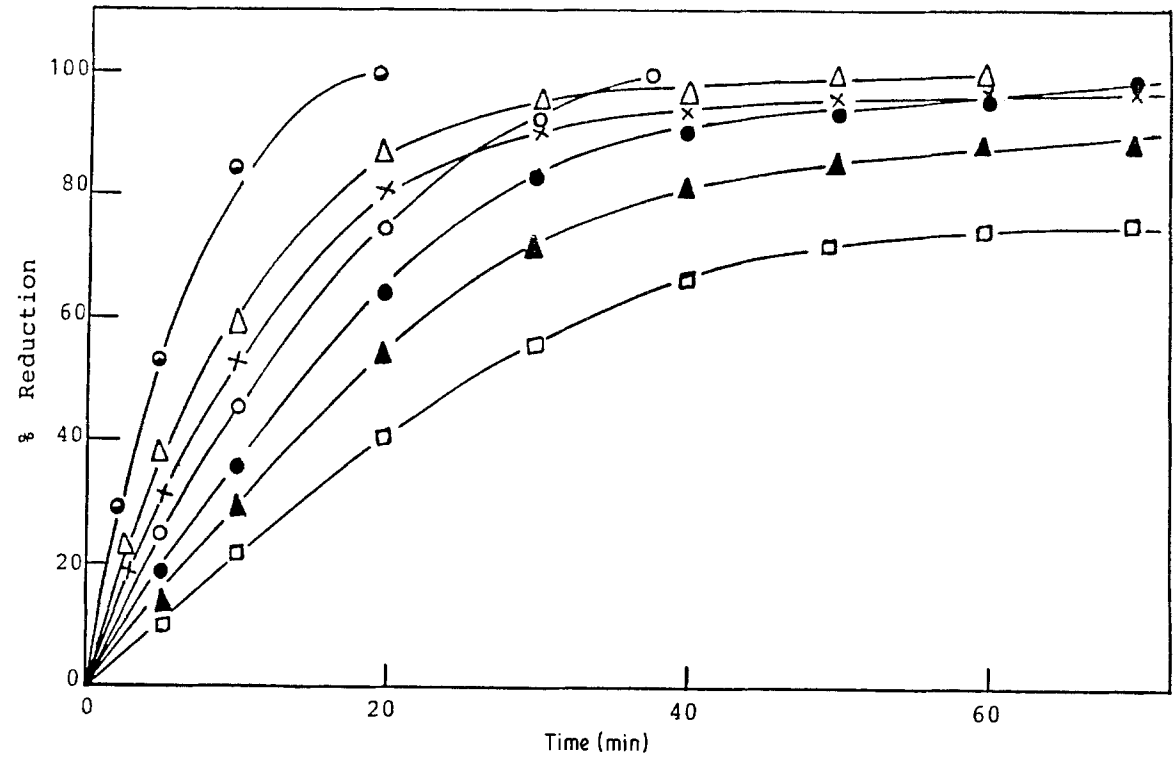

Figure 3 Reduction curves of Fe_2O_3 briquettes with 75% H_2 + 25% CO. Reduction temperatures as in Fig. 2.

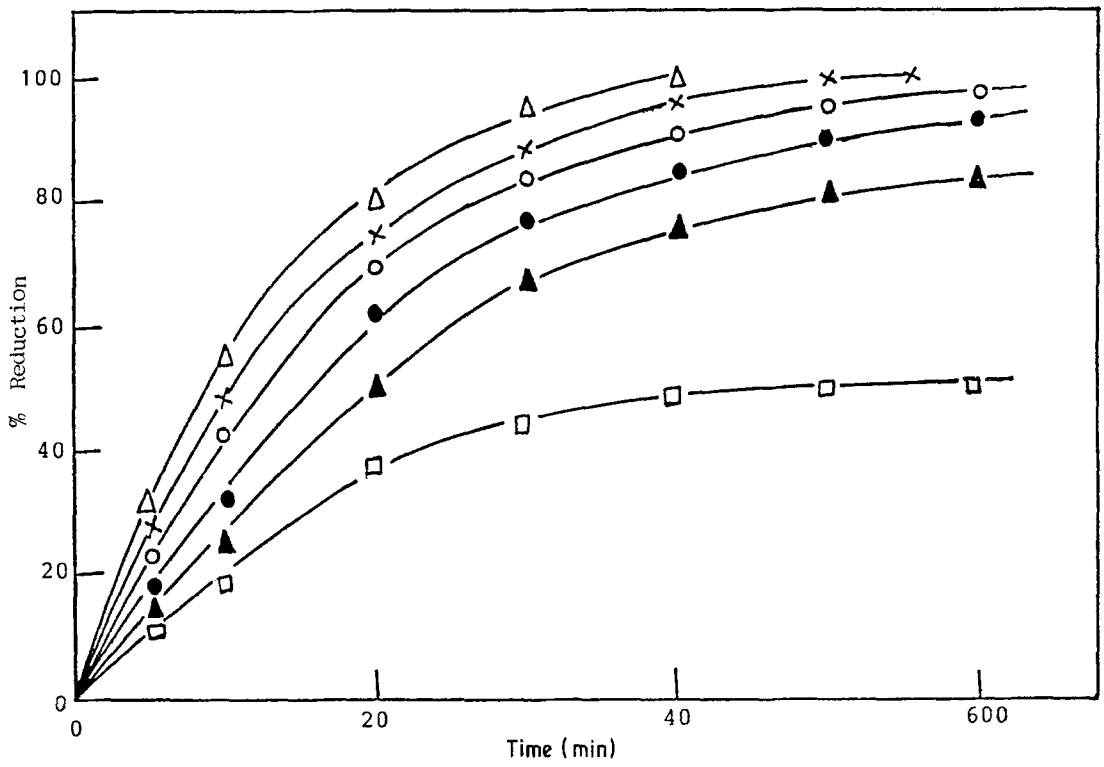

Figure 4 Reduction curves of Fe_2O_3 briquettes with 50% H_2 + 50% CO. Reduction temperatures (° C): △, 1000; ×, 950; ○, 900; ●, 800; ▲, 700; □, 600.

respectively. It shows the slowing down of the reduction rate at 950 and 1000° C. In order to highlight this phenomenon more clearly, the computed values of the rate of reduction (dR/dt) at different extents of reduction (30, 70 and 95%) were calculated.

Fig. 7 shows the relationship between the rate of reduction (% min^{-1}) and the corresponding reduction temperature. It can be observed that, at 30% reduction, the rate increased with temperature. On the other hand, at 70 and 95% reduction, the rate increased with temperature up to 900° C, then decreased giving the lowest rate at 950° C after which the rate increased again. The slowing down of the reduction rate between 900 and 950° C can be attributed to either the formation of γ-iron on the surface of grains and/or sintering of the formed iron phase. At 912° C γ-iron is formed whereas α-iron is present below this temperature [16]. Under these conditions the gas diffusion is the rate-controlling process.

The diffusivity of reducing gasses (hydrogen and

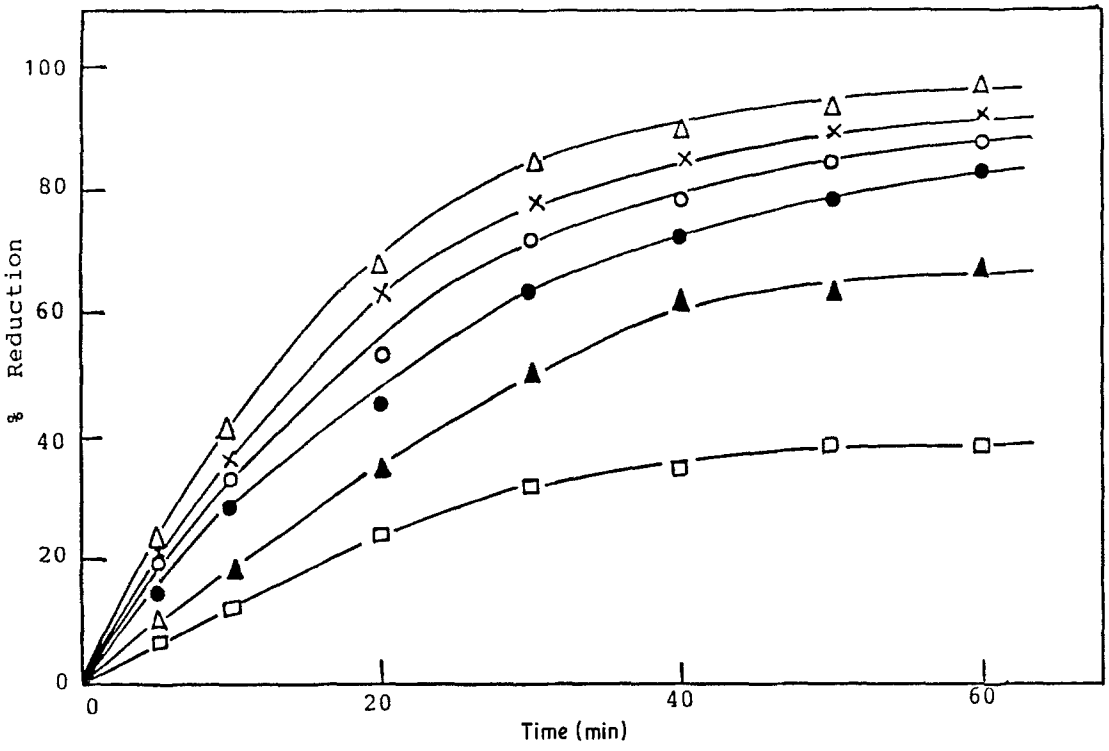

Figure 5 Reduction curves of Fe_2O_3 briquettes with 25% H_2 + 75% CO. Reduction temperatures as in Fig. 4.

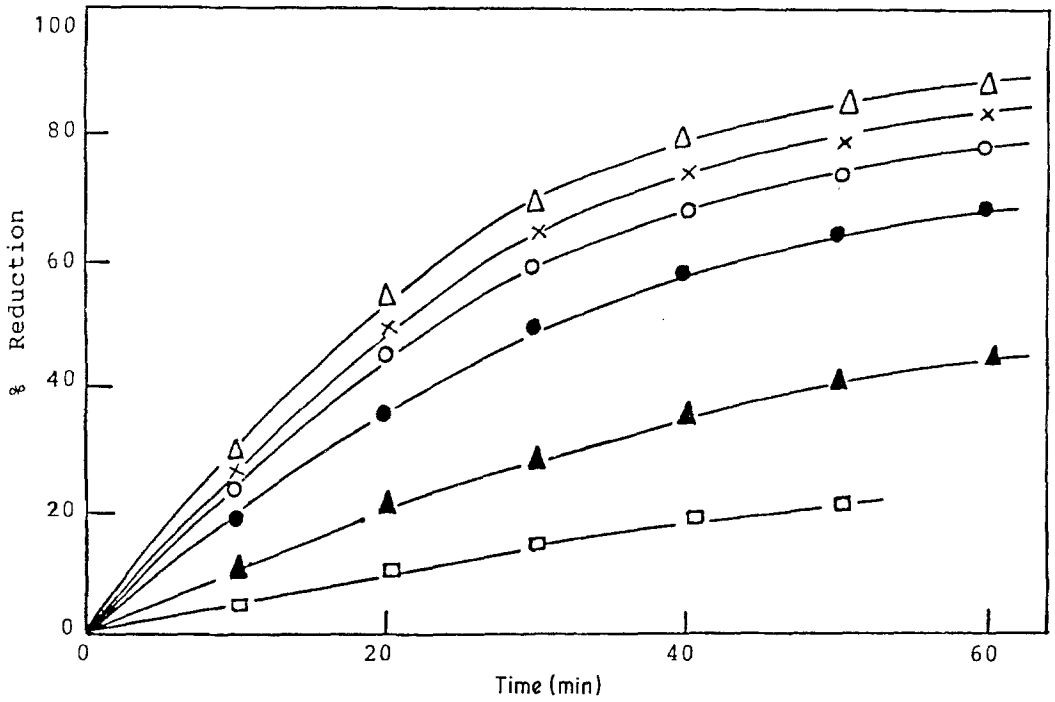

Figure 6 Reduction curves of Fe_2O_3 briquettes with CO. Reduction temperatures as in Fig. 4.

carbon monoxide) and the product gasses (steam and carbon dioxide) in γ-iron is much slower than that in the α-iron [7]. Accordingly, the rate of reduction (dR/dt) of iron oxide decreased at 900 to 950° C giving a reduction rate minimum. Sintering of the reduced iron, which increases with temperature, decreases the rate of reduction due to the lower rate of gas diffusion inside the former iron layer. Accordingly, at the minimum-rate temperature the mechanism of reduction can also be controlled by solid state diffusion.

After the reduction rate reaches a minimum value at 900 to 950° C, it gradually increases again with increasing temperature. Although the rise in temperature increases the ability of iron coatings to recrystallize and sinter (a matter which would decrease the reduction rate) it must be emphasized that the mobility and migration of holes and ions (solid-state diffusion) are also favoured with the rise in temperature which in turn favours the reduction rate. At 30% reduction extent the amount of metallic iron formed due to reduction at 900 to 950° C is so small that a very thin layer of iron cannot be nucleated all over the oxide surface and hence the rate of reduction increased with temperature.

The relationship between the total porosity of the reduced briquettes and the corresponding reduction temperature is shown in Fig. 8a. It indicates that with rise in temperature to 900° C the porosity increased after which it decreased until 950° C was reached, and then increased again. It would be expected that porosity increased gradually during reduction due to the removal of oxygen ions from the iron oxide lattice and the accompanied structural changes. At the minimum-rate temperature the rate of reduction is slower and consequently the rate of development of pores decreased resulting in a much more pronounced effect of sintering and recrystallization of iron. Accordingly the pores are sealed and a decrease in porosity at 900 to 950° C is obtained. Above 950° C the values of total porosity increased again due to the shorter time of reduction.

The microscopic appearance of partially reduced samples (70% reduction extent) at 900 and 950° C in hydrogen is shown in Figs 9a and b, respectively. At 900° C, Fig. 9a shows an iron–wustite zone which contains some wustite areas not completely entrapped in iron which is nucleated and grows on some parts of the oxide surface. Fig. 9b, at 950° C, shows that iron is nucleated on the whole surface of the oxide resulting in a large amount of entrapped wustite in dense iron films. The size of the iron nuclei formed can grow through further reduction and their thickness increases with time and temperature; they become dense through sintering and recrystallization, thus hindering further gas diffusion to and from the unreduced wustite relics. For this reason the reduction rate is greatly retarded at the minimum-rate temperature and the reduction mechanism can be controlled by solid state diffusion of the oxygen atoms in the iron layer. The rate of solid state diffusion and, consequently, the rate of reduction increases with temperature above 950° C.

3.1.2. Reduction with carbon monoxide and carbon monoxide-rich mixtures

The reduction of Fe_2O_3 briquettes with carbon monoxide-rich gas mixtures ($\geq 50\%$ CO), as given in Figs 4 to 6, shows an increase in the reduction rate with temperature. Below 800° C, the reduction was stopped before completion, depending on the carbon monoxide content in the gas mixture. This was due to the amount of carbon deposition resulting from the thermal decomposition of carbon monoxide ($2CO \rightleftharpoons CO_2 + C$) being greater than the rate of oxygen removal due to reduction in the later stages. Table I shows the total amount of carbon in the reduced briquettes at 900 to 1050° C and the corresponding reduction time. It can be seen from Table I that the

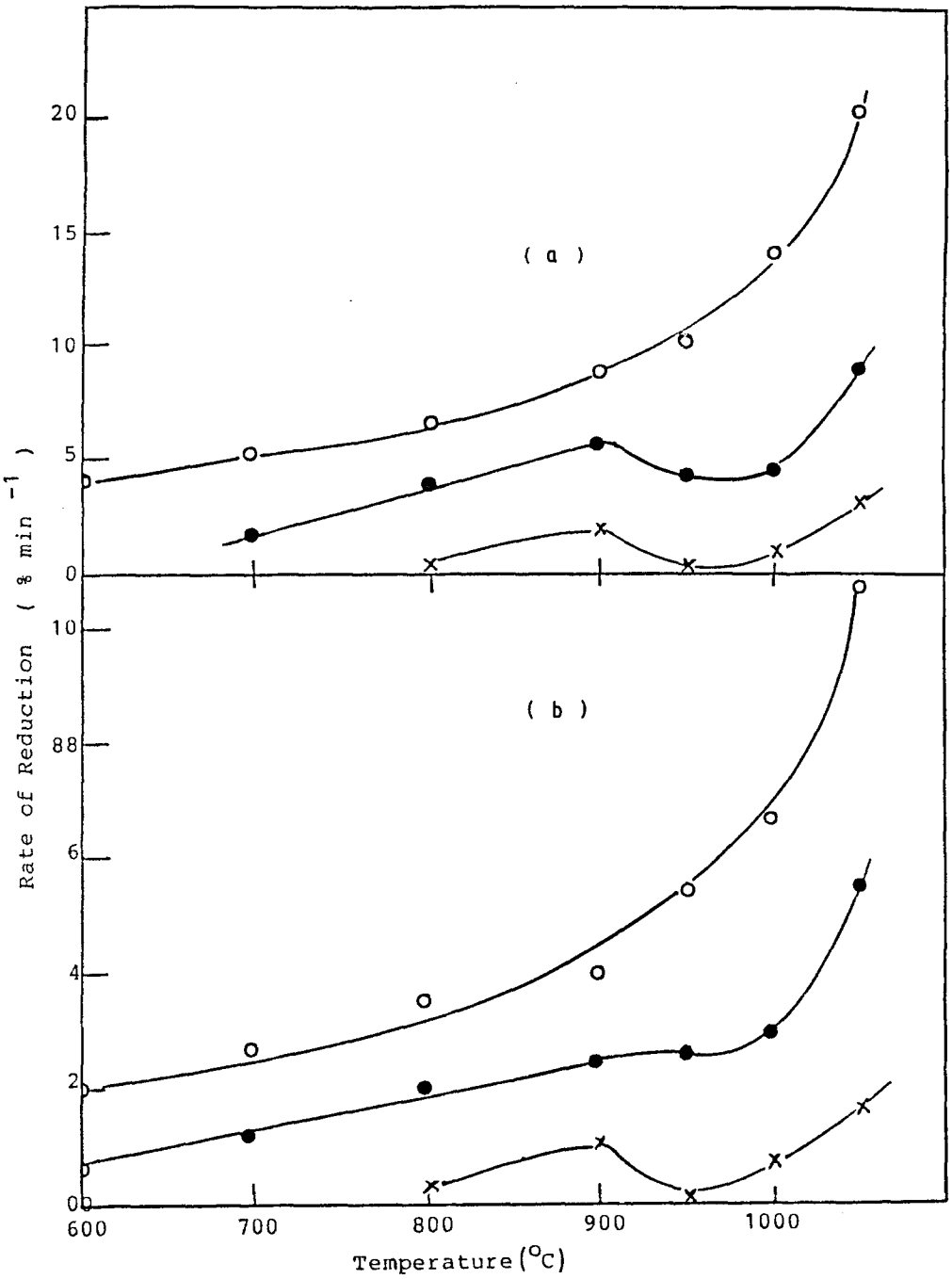

Figure 7 Variation of reduction rate with temperature. Reduction (a) with hydrogen, (b) 75% H_2 + 25% CO. Reduction extent (%): o, 30%; ●, 70%; x, 95%.

carbon content in the reduced samples increased with time and decreased with temperature for a given reducing gas mixture. It also increased with increase in the carbon monoxide content in the gas mixture. At 950 and 1000° C, in the case of reduction with 50% H_2 + 50% CO mixture, the carbon content in the reduced sample decreased more than in the 75% H_2 + 25% CO mixture due to the shorter reduction time in the former than the latter. This indicates that the time of reduction has a greater influence on the rate of carbon deposition than the carbon monoxide content of the gas mixture.

X-ray diffraction analysis of these samples showed the presence of cementite (Fe_3C) and α-Fe. Chemical

TABLE I Carbon content in the reduced Fe_2O_3 briquettes and the reduction time

Reducing gas (%)		9000° C		950° C		1000° C		1050° C	
H_2	CO	t_{min}	% C	t_{min}	% C	t_{min}	% C	t_{min}	% C
100	–	20	–	50	–	30	–	12	–
75	25	38	0.62	80	0.81	60	0.52	20	0.08
50	50	80	0.85	55	0.62	40	0.40	30	0.17
25	75	120	1.10	90	0.89	65	0.58	42	0.29
–	100	150	1.72	120	1.10	80	0.72	65	0.38

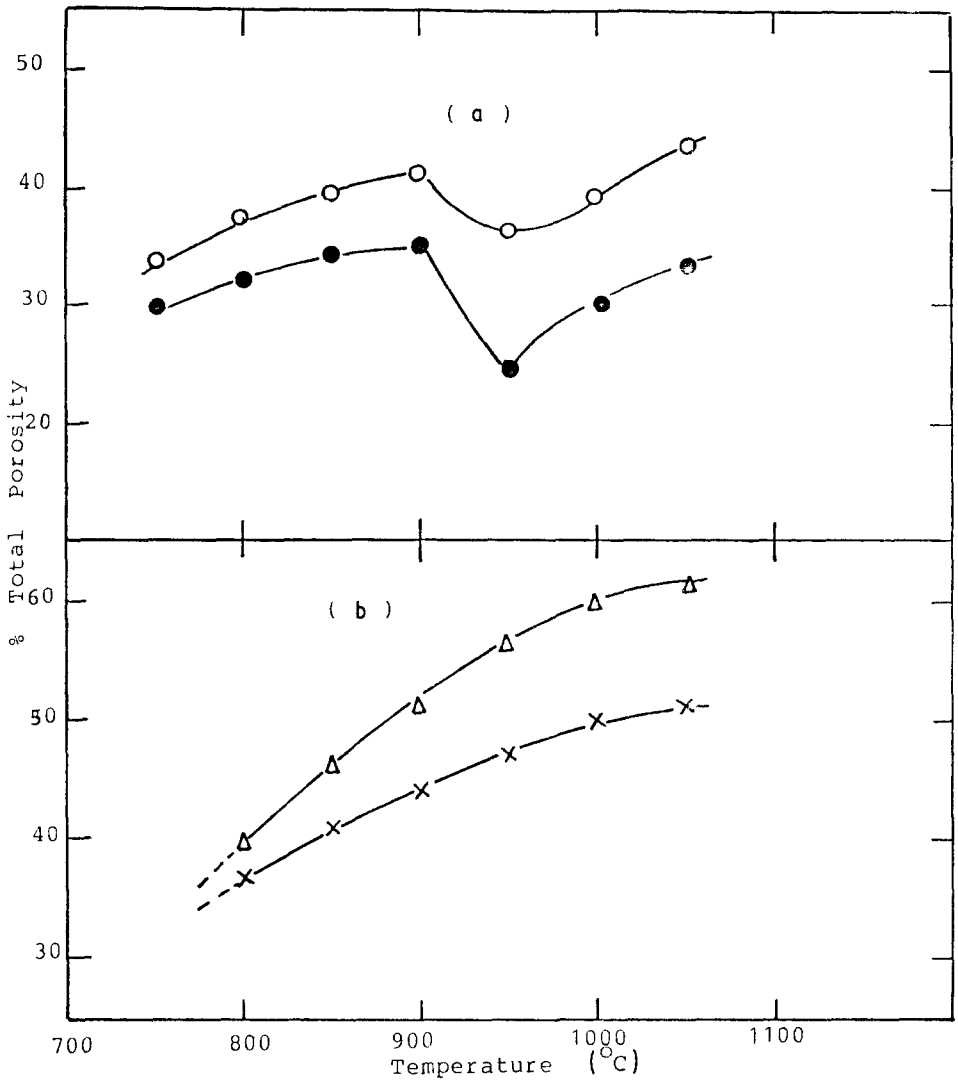

Figure 8 Variation between total porosity of completely reduced samples and reduction temperature. Reducing gases: (a) ○, 100% H_2, ●, 75% H_2 + 25% CO; (b) △, 50% H_2 + 50% CO, ×, 100% CO.

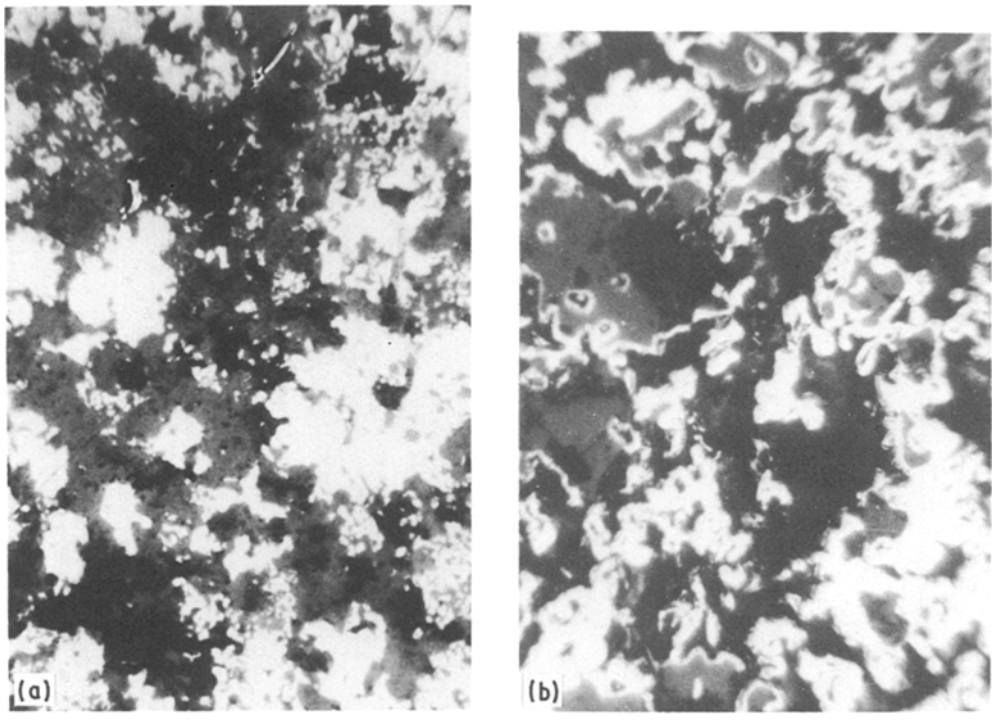

Figure 9 Photomicrographs of partially reduced samples with hydrogen: (a) at 900° C; (b) at 950° C. × 180.

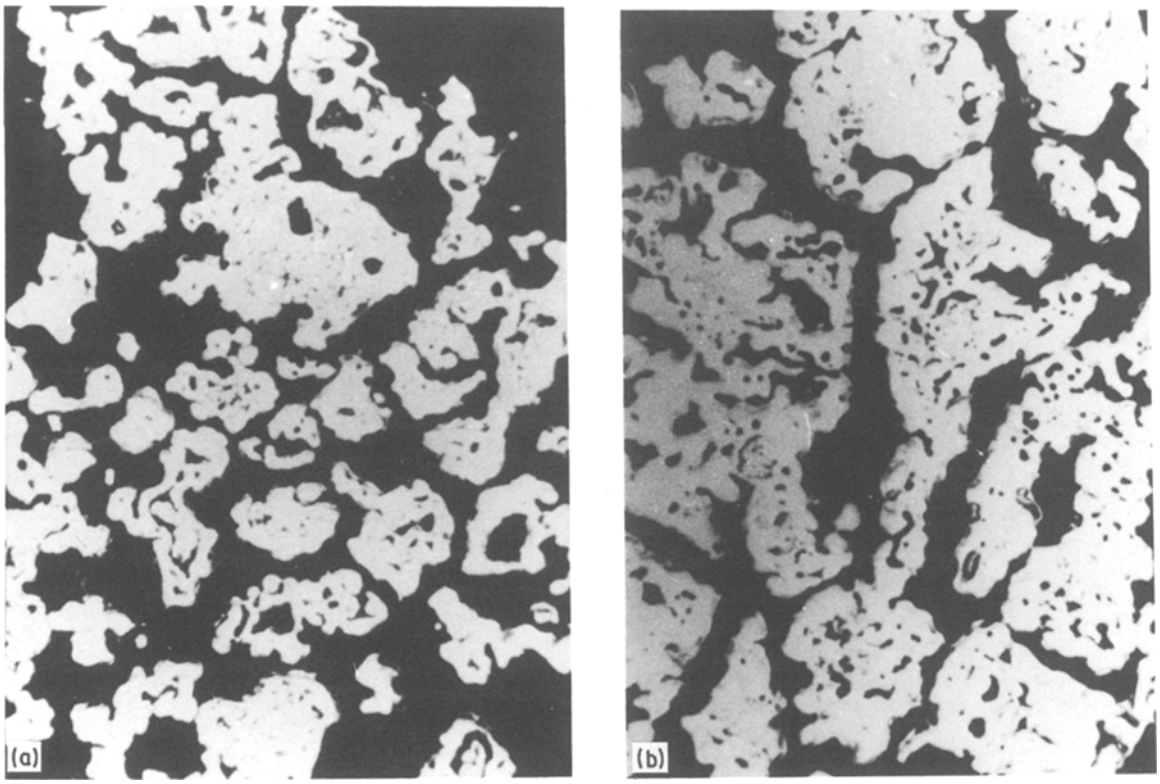

Figure 10 Photomicrographs of completely reduced samples at 1000° C: (a) with carbon monoxide; (b) with hydrogen, x 180.

analysis of the reduced samples indicated that free carbon was also present in addition to Fe_3C especially at lower temperatures $< 900°$ C. Iron carbides and free carbon can be formed by the following reactions [10]:

$$2(CO)_g \rightleftharpoons 2(CO)_{ads} \rightleftharpoons CO_{2(g)} + C_{gr} \quad (1)$$

This carbon can react with either metallic iron or lower oxide (FeO) as follows:

$$(C)_{gr} + 3Fe \rightarrow Fe_3C \quad (2)$$

$$(C)_{gr} + 2FeO \rightarrow 2Fe + CO_2 \quad (3)$$

At higher temperatures $> 900°$ C, the reaction between

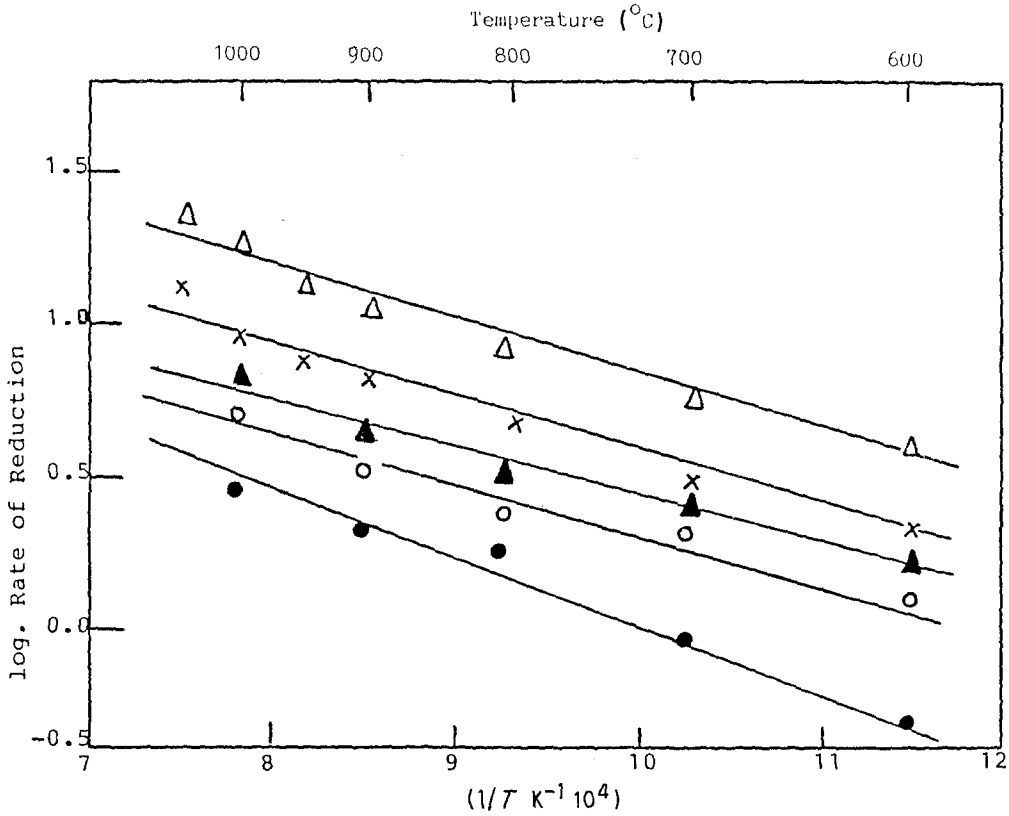

Figure 11 Arrhenius plots for the reduction of Fe_2O_3 briquettes in the initial stages of reduction. Reducing gas compositions: △, 100% H_2; ×, 75% H_2 + 25% CO; ▲, 50% H_2 + 50% CO; ○, 25% H_2 + 75% CO; ●, 100% CO.

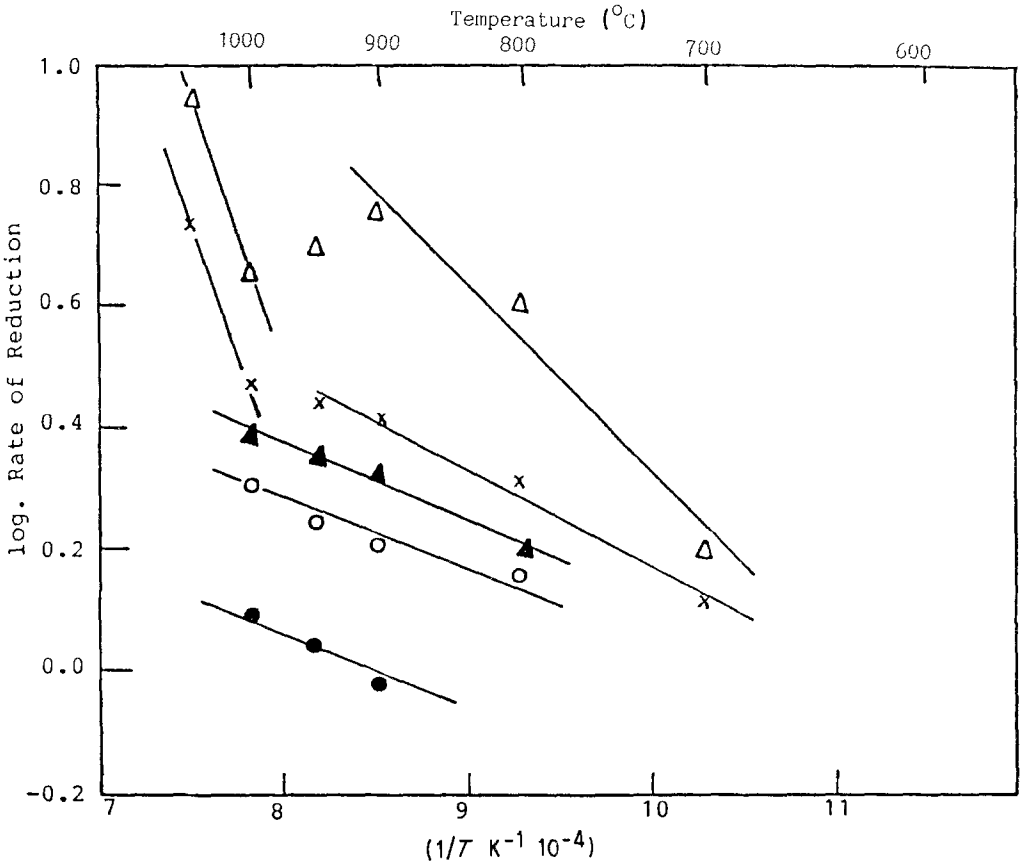

Figure 12 Arrhenius plots for the reduction of Fe_2O_3 briquettes in later stages of reduction. Reducing gas compositions as in Fig. 11.

Fe_3C and FeO can take place;

$$2FeO + Fe_3C \rightarrow 5Fe + CO_2 \quad (4)$$

Unlike hydrogen and hydrogen-rich gas mixtures the reduction with carbon monoxide-rich gas mixtures ($\geqslant$ 50% CO) and with pure carbon monoxide showed no rate minimum during reduction at 600 to 1050° C as shown in Figs 4 to 6. This was attributed to the carbon deposition and the side reactions (Reactions 1 to 3). The presence of carbon between iron grains counteracts their sintering and sticking together. Accordingly the temperature at which sintering occurs is higher than that in hydrogen and hydrogen-rich gas mixtures [8]. This was indicated by the absence of wustite relics in the case of reduction with 50% H_2 + 50% CO mixture. Moreover, the completely reduced samples with carbon monoxide and carbon monoxide-rich gas mixtures, showed that the iron grains formed are burst in the briquettes, giving a large number of smaller grains as shown in Fig. 10a, while more sintering was observed for the reduction with either hydrogen or hydrogen-rich mixtures (Fig. 10b).

The bursting of iron particles in carbon monoxide and carbon-rich mixtures was previously discussed [10] in the light of side reactions to form carbon dioxide (Reactions 1, 3 and 4) which build-up high pressure at the FeO/Fe interface. The resulting pressure may reach 4 to 5 atm, above which the grains burst [17]. On the other hand, in hydrogen the steam formed at an interface does not reach a fraction of atomospheric pressure. Therefore, sintering is expected in hydrogen while bursting of particles during carbon monoxide reduction is considered [10].

Porosity measurements of the reduced briquettes in carbon monoxide and 50% H_2 + 50% CO mixture at 900 to 1050° C as shown in Fig. 8b, confirm this explanation. They show that higher porosity was obtained in carbon monoxide reduction than that in H_2–CO mixtures at all temperatures and the difference inceases with temperature. This also indicates that more bursting and less sintering effect is observed in carbon monoxide reduction. On the other hand, the presence of hydrogen enhanced sintering and recrystallization of iron resulted in a lower porosity of the reduced iron.

3.1.3. Temperature dependence of the reduction rate

The apparent activation energy (E_a) for the reduction of Fe_2O_3 briquettes with hydrogen, carbon monoxide and H_2–CO mixtures was calculated from the Arrhenius equation:

$$K_r = K_0 e^{E_a/RT} \quad (5)$$

where K_r is the rate constant and K_0 is the frequency factor. A true activation energy reflects the energy barrier associated with the rate-determining step. The relationship between the logarithm of the reduction rate in the initial stages (5%) and at later stages (70%) and the reciprocal of the absolute temperature are shown in Figs 11 and 12, respectively. The computed values of E_a obtained from these plots are given in Table II.

It can be seen from Table II that, in the initial stages of reduction, the value of E_a increased with increasing amount of carbon monoxide in the gas mixture giving the highest value in pure carbon monoxide. This

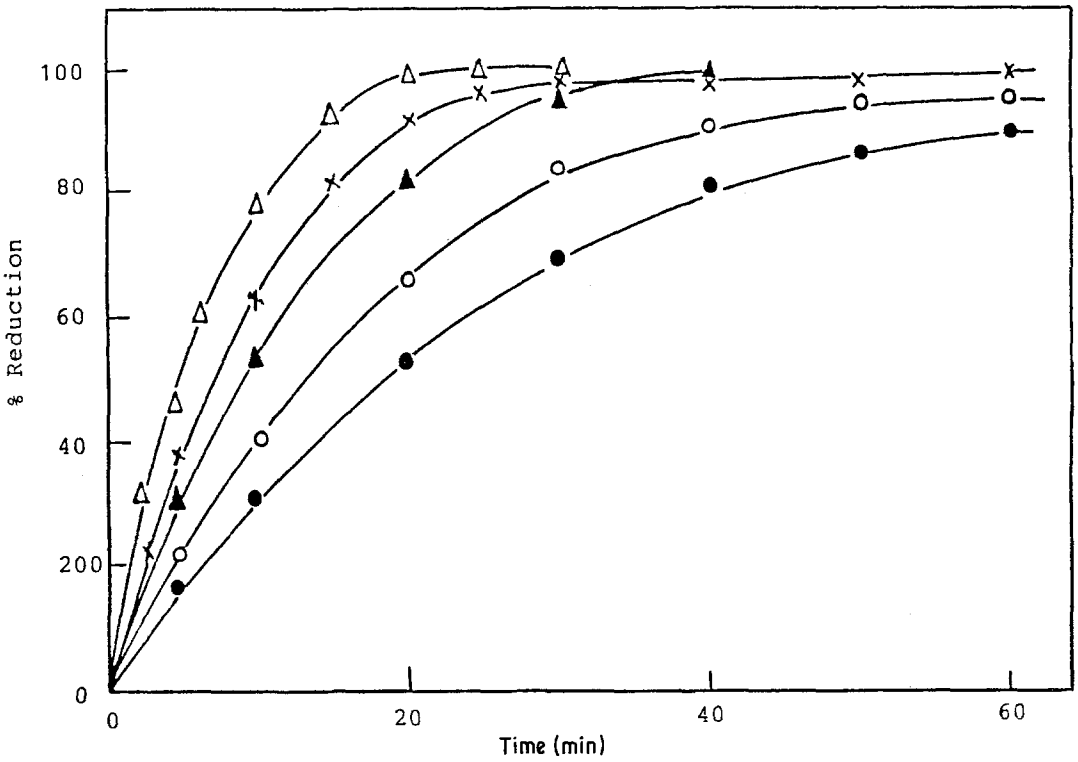

Figure 13 Influence of reducing gas compositions (as given in Fig. 11) on the reduction of Fe_2O briquettes at 1000° C.

reflects that hydrogen can more easily diffuse and react with Fe_2O_3 than can carbon monoxide. The smaller molecular diameter of hydrogen (0.074 nm) than carbon monoxide (0.113 nm) also accounts for easier diffusion of its molecules.

The values of the apparent activation energy obtained are gradually increased from 6.87 kcal mol^{-1} in pure hydrogen to 13.50 kcal mol^{-1} in pure carbon monoxide depending on the carbon monoxide content in the gas mixture. This reveals that the rate-controlling mechanism is changed from gas diffusion in hydrogen to interfacial chemical reaction in carbon monoxide, whereas in H_2–CO mixtures, a combined effect of both mechanisms is considered.

In the later stages of reduction (70% reduction extent) on the other hand, the values of E_a obtained showed that it is temperature dependent:

(a) at $\leqslant 900°$ C the values of E_a decreased from 14.20 kcal mol^{-1} in hydrogen to 5.28 kcal mol^{-1} in CO. In H_2–CO mixtures, the E_a decreased with increase in the carbon monoxide content in the gas mixture. This indicates that the mechanism of reduction changes from interfacial chemical reaction in hydrogen to gas diffusion in carbon monoxide. This can be attributed to the carbon deposition and its secondary reactions (Reactions 1 to 4). This will enhance bursting of the iron layer which, in turn, facilitates gas diffusion to and from the unreduced particles. Therefore, the reaction-controlling mechanism is changed to gas diffusion. The contribution of gas diffusion to the rate-controlling process is dependent on the carbon monoxide content in the gas mixture;

(b) at $\geqslant 950°$ C, the calculated values of the apparent activation energy in hydrogen and 75% H_2 + 25% CO gas mixture are 40.30 and 37.56 kcal mol^{-1}, respectively. These values reveal that the solid-state diffusion mechanism is the rate-determining step in the later stages of reduction. This was also confirmed by the presence of entrapped wustite relics as shown in Fig. 8b.

3.2. Influence of reducing gas composition

The isothermal reduction of Fe_2O_3 briquettes was carried out at 600 to 1050° C in hydrogen, carbon monoxide and H_2–CO mixtures (Figs 2 to 6). The effect of reducing gas composition on the reducibility of iron oxide was also studied. Fig. 13 shows the reduction curves at 1000° C, as an example, in hydrogen, carbon monoxide and their mixtures. It shows that in the early stages of reduction the highest rate was observed in hydrogen while the slowest was in carbon monoxide. For the reduction with H_2–CO mixtures, a combined effect of both gasses was obtained. As the carbon monoxide content in the gas

TABLE II Apparent activation energy (kcal mol^{-1}) as a function of reducing gas composition at 5 and 70% reduction extent

Reducing gas (%)		E_a at 5% reduction, 700 to 1050° C	E_a at 70% reduction	
H_2	CO		700 to 900° C	950 to 1050° C
100	–	6.87	14.20	40.30
75	25	7.79	11.80	37.56
50	50	8.70	7.95	7.95
25	75	10.81	6.40	6.40
–	100	13.50	5.28	5.28

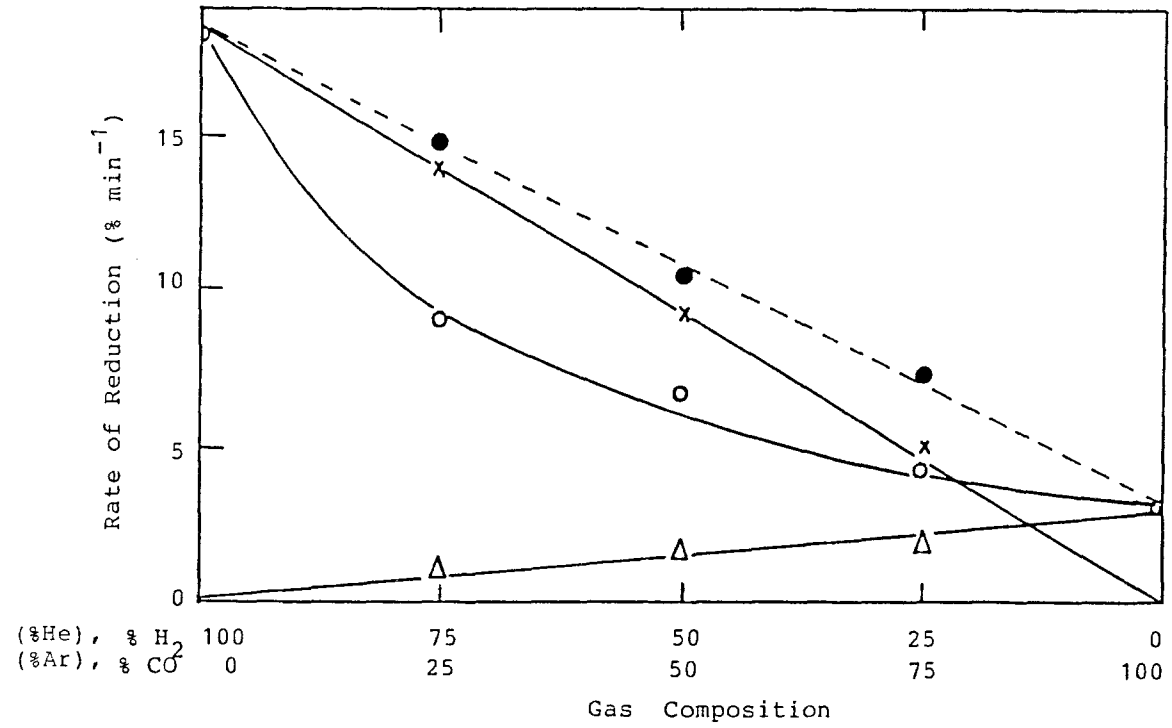

Figure 14 Variation of the initial rate of reduction at 1000° C with the reducing gas composition: ×, H_2–Ar mixtures; ○, H_2–CO mixture; △, He–CO mixture; ●, calculated from Equation 6.

mixture increases, the corresponding reduction rate decreases. The relative contribution of each gas (hydrogen or carbon monoxide) in the reduction process depends mainly on their activity and selective adsorption on the iron oxide surface.

In order to study the influence of either hydrogen or carbon monoxide individually in their mixture on the reducibility of Fe_2O_3, hydrogen was replaced by helium while carbon monoxide was replaced by argon in H_2–CO mixtures, i.e. the reduction was carried out with H_2–Ar and He–CO gas mixtures at 1000° C. In this case the reduction of Fe_2O_3 was conducted with hydrogen or carbon monoxide at different partial pressures (P_{H_2}, P_{CO}) since helium or argon in the mixtures act as inert gases. Fig. 14 shows the relationship between the rate of reduction (dR/dt) at their initial stages at 1000° C and the reducing gas composition. It shows that linear relationships were obtained in H_2–Ar and He–CO gas mixtures. As P_{H_2} decreased the corresponding rate of reduction decreased. On the other hand, in the case of reduction with H_2–CO mixtures, the linear relationship was not obtained, moreover a decrease in the rate was observed with increase in the carbon monoxide content in the gas mixture. Fig. 14 also shows the calculated rate of reduction obtained by applying the additive equation:

$$R_{H_2\text{-CO mix.}} = \dot{R}_{H_2} X_{H_2} + \dot{R}_{CO} X_{CO} \quad (6)$$

where $\dot{R}_{H_2}$, $\dot{R}_{CO}$ are the rates in pure hydrogen and pure carbon monoxide, whilst X_{H_2}, X_{CO} are the mole fractions of hydrogen and carbon monoxide in H_2–CO mixtures.

The results in Fig. 14 shows a greater decrease in the rates obtained during reduction with H_2–CO mixtures than the values calculated and even less than that in H_2–Ar gas mixtures. This clearly indicates that the presence of carbon monoxide in H_2–CO mixtures, even in small amounts, greatly retarded the reduction process. The difference between the experimental and the calculated rates of reduction increases with decrease in the carbon monoxide content in the gas mixtures which indicates that the presence of carbon monoxide in the mixture has a negative effect on the reduction rate of Fe_2O_3.

In previous work [9] a similar observation was detected during reduction of wusite micropellets with hydrogen, carbon monoxide and their mixtures. This was attributed to chemisorption of carbon monoxide molecules on some sites of the oxide surface. The surface coverage by carbon monoxide molecules will hinder the reduction by hydrogen resulting in a slowing of the rate. As the carbon monoxide content in the mixture increases, the surface coverage will increase leading to further slowing in the reduction rate. Unlike carbon monoxide, the addition of hydrogen to carbon monoxide enhanced the reduction of Fe_2O_3 due to the fact that hydrogen can more easily be chemisorbed and reacted with oxygen in the iron oxide than carbon monoxide. The easier diffusion of hydrogen than carbon monoxide also plays a part in enhancing the rate of reduction. This will lead to the formation of a large number of iron nuclei on the surface of the oxide which can further grow under the combined effect of both gases. In the later reduction stages, reduction with carbon monoxide and with carbon monoxide-rich gas mixtures ($\geqslant 50\%$ CO) is much faster than in hydrogen and hydrogen-rich gas mixtures ($> 50\%$ H_2). This was attributed to carbon deposition and its secondary reactions.

4. Conclusions

Fe_2O_3 briquettes were reduced at 600 to 1050° C in hydrogen, carbon monoxide and their mixtures. The kinetics and mechanisms of reduction were studied

using X-ray and carbon analyses and microscopic examinations of either partially or completely reduced samples.

In hydrogen and hydrogen-rich gas mixtures, a slowing down in the rate of reduction was detected at 900 to 950° C and was attributed to either α–γ-transformation of metallic iron and/or sintering of the iron phase. In carbon monoxide and carbon monoxide-rich gas mixtures this rate minimum was eliminated due to the bursting of the reduced grains. This bursting resulted from the carbon deposition and its side reactions producing carbon dioxide under high pressure at the Fe/FeO interface. The values of activation energy obtained (5 to 40 kcal mol^{-1} reveal different reaction mechanisms ranging from gas diffusion to solid-state diffusion.

The influence of the addition of one gas (hydrogen or carbon monoxide) to the other was investigated by using He–CO and H_2–Ar gas mixtures for reduction of Fe_2O_3. This showed that the presence of carbon monoxide with hydrogen greatly decreased the rate in the initial stages due to a poisoning effect, and enhanced the rate in the later stages due to the side reactions of deposited carbon.

References

1. C. G. DAVIS, J. F. McFARLIN and H. R. PRATT, *Ironmaking and Steelmaking* **9** (3) (1982) 93.
2. L. V. BOGDANDY and J. J. ENGELL, "The reduction of iron ores" (Springer Verlag, Berlin, 1971).
3. E. T. TURKDOGAN and J. V. VINTERS, *Met. Trans.* **2** (1971) 3175.
4. *Idem, ibid.* **3** (1972) 1561.
5. A. P. PROSSER, Influence of mineralogical factors on the rates of chemical reaction of minerals, in "Mineral processing and extractive metallurgy" (IMM, London, 1970) p. 59. 9th Commonwealth Mineral Metallurgy Congress (1969) Vol. 3.
6. K. A. SHEHATA and S. Y. EZZ, *Trans. IMM* **82C** (1973) 638.
8. A. A. EL-GEASSY, K. A. SHEHATA and S. Y. EZZ, *Trans. ISIJ* **17** (1977) 629.
9. A. A. EL-GEASSY and V. RAJAKUMAR, *ibid.* **25** (1985) 449.
10. *Idem, ibid.* **25** (1985) 1202.
11. A. A. EL-GEASSY, *ibid.* **25** (1985) 1036.
12. K. A. SHEHATA, A. A. EL-GEASSY and M. I. NASR, *J. Iron Steel Int.* **55** (1982) 45.
13. A. A. EL-GEASSY, K. A. SHEHATA and S. Y. EZZ, *ibid.* **49** (1976) 427.
14. *Idem, ibid.* **50** (1977) 329.
15. P. K. STRONGWAY, MSc thesis, University of Toronto (1964).
16. H. L. SAUNDTESS and H. J. TRESS, *J. Iron Steel. Inst.* **152** (1945) 291.
17. K. BOHNENKAMP, E. RIECKE and H. J. ENGELL, *Arch. Eisenhüttenw.* **38** (1967) 249.

Received 18 March 1985
and accepted 21 January 1986